

# Interference effects in Laue diffraction of Mössbauer $\gamma$ radiation in a $\text{Fe}_3\text{BO}_6$ crystal

I. G. Tolpekin, P. P. Kovalenko, V. G. Labushkin, E. N. Ovchinnikova, É. R. Sarkisov, and E. V. Smirnov

*All-Union Scientific-Research Institute of Physicotechnical and Radio Engineering Measurements, Mendeleevo, Moscow Province*

(Submitted 15 June 1987)

Zh. Eksp. Teor. Fiz. **94**, 329–343 (February 1988)

Diffraction of 14.4-keV Mössbauer  $\gamma$  radiation in a  $^{57}\text{Fe}_3\text{BO}_6$  single crystal was investigated in the Laue geometry. An analysis was made of how a spin-reorientation phase transition in a crystal affected the interference of resonance nuclear scattering of  $\gamma$  radiation by  $^{57}\text{Fe}$  nuclei occupying crystallographically inequivalent  $4c$  and  $8d$  positions. Reflection spectra of the  $(00l)$  and  $(0k0)$  types were determined experimentally both for purely nuclear  $\gamma$  scattering and in the presence of interference between resonant nuclear and Rayleigh electron scattering of  $\gamma$  photons. Resonance peaks due to a hyperfine combined interaction in  $\text{Fe}_3\text{BO}_6$  were observed in  $(001)$  and  $(003)$  reflection spectra. In the case of destructive interference of the scattering by the  $^{57}\text{Fe}$  nuclei at the  $4c$  and  $8d$  positions the intensity of the diffracted beam could be enhanced by interference (interference bleaching of the crystal). The experimental spectra were in agreement with the results of numerical calculations carried out for a perfect crystal.

## 1. INTRODUCTION

Interference effects which occur in the course of diffraction of Mössbauer  $\gamma$  radiation in crystals can have a considerable influence on the diffraction pattern, particularly on the nature of the energy spectra of the diffracted  $\gamma$  radiation (see, for example, Refs. 1–3). They include interference between resonance nuclear and Rayleigh electron scattering of  $\gamma$  photons, interference in scattering via different transitions between the Zeeman sublevels of the ground and excited states of the nuclei, etc.

Studies of interference effects in diffraction scattering of Mössbauer gamma radiation in crystals, in which resonating nuclei occupy crystallographically inequivalent positions in a unit cell, are of great current interest. For example, Refs. 4 and 5 report investigations of interference of Mössbauer gamma radiation scattered by  $^{57}\text{Fe}$  nuclei located at  $4c$  special and  $8d$  general positions in a  $^{57}\text{Fe}_3\text{BO}_6$  crystal (interference between  $c$  and  $d$  resonance lines). It was found that, depending on the signs of the structure factors of the iron nuclei at the  $4c$  and  $8d$  positions, interference could be constructive or destructive, and it was demonstrated that interference narrowing of a resonance line was possible and also that the interference pattern was highly sensitive to details of the magnetic structure of a crystal.

An analysis of the influence of interference between the  $c$  and  $d$  lines on the spectra of the Bragg scattering of Mössbauer  $\gamma$  radiation was analyzed in Refs. 4 and 5. It would be of considerable interest to study diffraction of Mössbauer radiation by a  $\text{Fe}_3\text{BO}_6$  crystal in the Laue geometry because the spectra should be influenced significantly by interference, as well as by resonance absorption of  $\gamma$  photons in a crystal, and also by the suppression of inelastic channels of nuclear reactions (the Kagan–Afnas'ev effect).<sup>1,6–8</sup>

An important feature which distinguishes a  $\text{Fe}_3\text{BO}_6$  crystal from other objects used in Mössbauer diffraction experiments is the presence of magnetic and inhomogeneous electric hyperfine fields at the crystal lattice sites and, since the energies of the interaction of these fields with the reson-

ating nuclei are comparable, qualitatively new results may be obtained for diffraction scattering of Mössbauer  $\gamma$  radiation.<sup>9,10</sup>

A  $\text{Fe}_3\text{BO}_6$  crystal belongs to the  $D_{2h}^{16}(Pnma)$  space group and is a two-sublattice antiferromagnet exhibiting weak ferromagnetism; the Néel point is  $T_N = 508$  K. A number of studies has been made (for a bibliography see Ref. 5) of the crystal and magnetic structures of this compound, and of the structure formed by electric field gradients (EFGs) at the Mössbauer nuclei. At a temperature  $T_{\text{SR}} = 415$  K a spin reorientation phase transition takes place in this crystal; in the range  $T < T_{\text{SR}}$  the antiferromagnetic axis is oriented along  $[001]$  and the weak ferromagnetic moment is along  $[100]$  whereas at  $T > T_{\text{SR}}$  the antiferromagnetic axis is along  $[100]$  and the weak ferromagnetic moment along  $[001]$ . The first investigations of the Laue diffraction of Mössbauer radiation in a  $\text{Fe}_3\text{BO}_6$  crystal<sup>11</sup> demonstrated that the diffraction spectra are very sensitive to spin reorientation in this crystal and revealed resonance peaks in the spectrum due to a combined hyperfine interaction.

Here we report the results of a systematic investigation of diffraction of Mössbauer  $\gamma$  radiation by a  $\text{Fe}_3\text{BO}_6$  crystal in the Laue geometry. In Sec. 2 we consider theoretically the influence of interference between the  $c$  and  $d$  lines on the intensity of the reflected radiation in the case of perfect and mosaic crystals. We describe the experimental method in Sec. 3 and provide details of a thermal chamber ensuring stabilization of the temperature of a crystal in the vicinity of  $T_{\text{SR}}$ . The results of experimental investigations of the energy spectra of the Laue reflections  $(001)$ ,  $(003)$ ,  $(002)$ , and  $(080)$  above and below the spin reorientation point  $T_{\text{SR}}$  are given and discussed in Sec. 4. We analyze the constructive and destructive interference between the  $c$  and  $d$  lines and of the combined hyperfine interaction in a  $\text{Fe}_3\text{BO}_6$  crystal on the nature of the diffracted radiation spectra. We compare the experimental spectra with those calculated theoretically for perfect and mosaic crystals.

## 2. SCATTERING OF MÖSSBAUER RADIATION IN A $\text{Fe}_3\text{BO}_6$ CRYSTAL; MODELS OF PERFECT AND MOSAIC CRYSTALS

We consider diffraction of Mössbauer  $\gamma$  radiation by a  $\text{Fe}_3\text{BO}_6$  crystal in the Laue geometry and determine how the interference between the processes of scattering by nuclei at inequivalent positions affects the nature of the angular and energy dependences of the diffracted beam intensity. We carry out this theoretical analysis allowing only for the magnetic structure of the crystal because the structure of EFGs is not yet known accurately (the results of Ref. 12 do not agree with the results of a symmetry analysis). The influence of this restriction on the agreement between the theoretical and experimental results will be discussed later.

The reflection coefficient of Mössbauer  $\gamma$  radiation incident on a perfect crystal in the form of a plane-parallel plate in the case of separable polarizations, which applies to all the experimental investigations reported in the present paper, is given by<sup>1</sup>

$$R_D^{s's} = 4 |F_{21}^{s's}|^2 \left| \exp\left(\frac{i\kappa\lambda_1^{s's}}{4\gamma_2} t\right) - \exp\left(\frac{i\kappa\lambda_2^{s's}}{4\gamma_2} t\right) \right|^2 \times |\lambda_1^{s's} - \lambda_2^{s's}|^{-2} \quad (1)$$

Here,

$$\lambda_{1,2}^{s's} = \frac{\gamma_2}{\gamma_1} F_{11}^{s's} + F_{22}^{s's} - \alpha \pm \left[ \left( \frac{\gamma_2}{\gamma_1} F_{11}^{s's} - F_{22}^{s's} + \alpha \right)^2 + 4 \frac{\gamma_2}{\gamma_1} F_{12}^{s's} F_{21}^{s's} \right]^{1/2},$$

where the rest of the notation is the same as in Ref. 13.

The amplitude  $F_{ij}^{s's}$  of coherent scattering of Mössbauer  $\gamma$  radiation by a unit cell in a  $\text{Fe}_3\text{BO}_6$  crystal is

$$F_{ij}^{s's} = F_{(N)ij}^{(c)s's} + F_{(N)ij}^{(d)s's} + F_{(R)ij}^{s's} \delta_{s's}, \quad (2)$$

where  $F_{(N)ij}^{(c)s's}$  and  $F_{(N)ij}^{(d)s's}$  are the amplitudes of the resonance scattering by the iron nuclei located at the 4c and 8d positions, respectively;  $F_{(R)ij}^{s's}$  is the Rayleigh amplitude of the scattering by atomic electrons; and  $\delta_{s's}$  is the Kronecker delta. The explicit form of the amplitudes  $F_{(N)ij}^{(c)s's}$  and  $F_{(N)ij}^{(d)s's}$  can be found in Ref. 5, whereas the amplitude  $F_{(R)ij}^{s's}$  is identical with the well-known amplitude for the scattering of x rays (see, for example, Ref. 14).

The expression (1) describes the dependence of the reflection coefficient  $R_D^{s's}$  on the angle of incidence on a crystal (parameter  $\alpha$ ). The corresponding angular dependence has been investigated in detail for the diffraction of x rays by weakly absorbing crystals. In the case of the diffraction of Mössbauer  $\gamma$  photons by a  $\text{Fe}_3\text{BO}_6$  crystal the reflection coefficient  $R_D$ , considered as a function of  $\alpha$ , is influenced strongly by the interference between the c and d lines, as well as by the resonant nuclear absorption of  $\gamma$  rays in the crystal.

We shall illustrate the dependence of  $R_D$  on  $\alpha$  given by Eq. (1) using the results of numerical calculations. Figure 1 shows the reflection curves of Mössbauer  $\gamma$  radiation of energy 14.4 keV for a  $\text{Fe}_3\text{BO}_6$  crystal in the case of scattering into the purely nuclear magnetic maximum (001). For this reflection the amplitude of the scattering at the Bragg angle  $F_{ij}^{s's}$  is governed by a sum of the first two terms in Eq. (2), since the Rayleigh amplitude  $F_{(R)ij}^{s's}$  ( $i \neq j$ ) vanishes for rea-

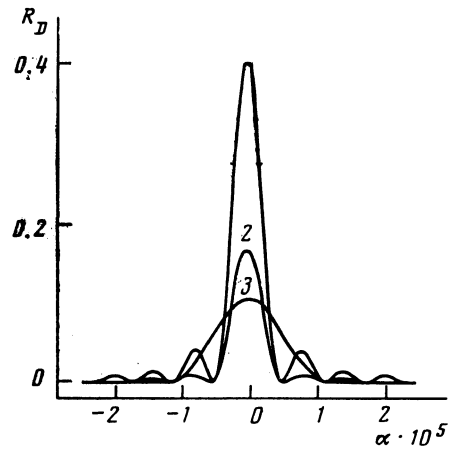


FIG. 1. Dependence of  $R_D$  on  $\alpha$  for the (001) reflection of Mössbauer radiation by a  $\text{Fe}_3\text{BO}_6$  crystal in the case of the following  $\gamma$ -photon energies: 1)  $E = E_0^d - 5\Gamma$ ; 2)  $E = E_0^d + 5\Gamma$ ; 3)  $E = E_0^d$ . The thickness of the crystal is 15  $\mu\text{m}$ .

sons of symmetry. The geometry of the scattering and the orientation of the antiferromagnetic axis in a crystal relative to the vectors  $\mathbf{k}_1$  and  $\mathbf{k}_2$  are given in Fig. 2. The structure factors  $F_{\text{str}}^c$  and  $F_{\text{str}}^d$  for the  $^{57}\text{Fe}$  nuclei at the 4c and 8d positions, respectively, are given in Table I. In the case of the (001) reflection the signs of  $F_{\text{str}}^c$  and  $F_{\text{str}}^d$  are identical, constructive interference takes place<sup>4,5</sup> and its influence on the form of  $R_D(\alpha)$  depends on the  $\gamma$  radiation energy  $E$ , i.e., on the position of  $E$  relative to the resonance values  $E_i^c$  and  $E_i^d$  for the c and d lines (here, the index  $i = 1, 2, \dots, 6$  labels the resonance lines in the spectrum of  $^{57}\text{Fe}_3\text{BO}_6$ ).

If  $E$  is close to the energy of an  $i$ th transition and the inequality  $E > \max(E_i^c, E_i^d)$  or  $E < \min(E_i^c, E_i^d)$  is obeyed, the real parts of the scattering amplitudes for the resonant nuclei at the 4c and 8d positions  $F_{(N)ij}^{(c)}$  and  $F_{(N)ij}^{(d)}$  add up, which enhances the diffraction reflection (curve 1 in Fig. 1). In this case the reflection coefficient  $R_D$ , considered as a function of  $\alpha$ , has a strong central peak reaching its maximum at  $\alpha = 0$  and its wings have clear side maxima (pendellösung beats with respect to the angle of incidence<sup>14</sup>). In the range of energies between the resonance values of  $E_i^c$  and  $E_i^d$  the real parts of  $F_{(N)ij}^{(c)}$  and  $F_{(N)ij}^{(d)}$  have opposite signs, which reduces the resultant scattering ampli-

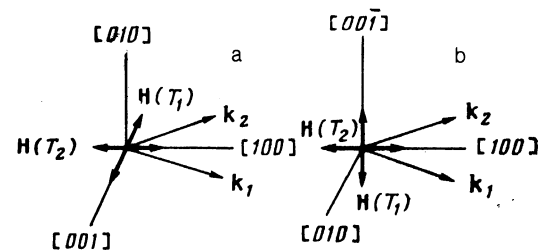


FIG. 2. Geometry of the scattering of Mössbauer radiation in a  $\text{Fe}_3\text{BO}_6$  crystal: a) (00l) reflection; b) (0k0) reflection at temperatures  $T_1 < T_{\text{SR}}$  and  $T_2 > T_{\text{SR}}$ . Here,  $\mathbf{H}(T_i)$  describes the orientations of the magnetic fields at the iron nuclei. The  $(\mathbf{k}_1, \mathbf{k}_2)$  plane is perpendicular to the plane of the figure.

TABLE I. Structure factors  $F_{\text{str}}^c$  and  $F_{\text{str}}^d$  reduced to one nucleus.

	Reflection			
	(001)	(002)	(003)	(080)
$F_{\text{str}}^c$	0.988	0.950	0.890	1.000
$F_{\text{str}}^d$	0.992	0.970	0.933	-0.994

tude and weakens the intensity of the reflected radiation (Fig. 2). The intensities of the central and side maxima are found to be considerably smaller than in the former case.

The influence of  $\gamma$  ray absorption on the nature of the dependence  $R_D(\alpha)$  was studied by calculations at the exact resonance when  $E = E_0^d$  (curve 3). They show that in this case the value of  $R_D$ , considered as a function of  $\alpha$ , exhibits a single peak of width greater than the width of the central peaks of curves 1 and 2, but of smaller amplitude. The pendellösung beats were absent from curve 3 because of the strong resonance absorption of  $\gamma$  photons in a crystal. It should be pointed out that the intensity integrated over the angle, governed by the area under the reflection curve, is stronger in case 3 than in case 2, but weaker than in case 1. A similar analysis of the dependence of  $R_D$  on  $\alpha$  can be carried out for the case of destructive interference, when  $F_{\text{str}}^c$  and  $F_{\text{str}}^d$  have opposite signs. Then the diffraction scattering is enhanced in the region between  $E_i^c$  and  $E_i^d$  and weakened outside it.

The results of this analysis apply in the case of ideal collimation of the incident beam. If the divergence of the beam exceeds the angular dimensions of the diffraction reflection region, the experimental intensity must be described by integrating Eq. (1) with respect to  $\alpha$ . Then, the characteristic features of the  $R_D$  due to the interference between the  $c$  and  $d$  lines will be manifested in the energy dependence of the reflection coefficient integrated over the angle.

We shall now consider diffraction of Mössbauer  $\gamma$  radiation in a mosaic crystal. We shall assume, as usual, that this crystal consists of a large number of slightly misoriented blocks (crystallites), which scatter noncoherently, and that attenuation of the incident beam by the scattering and absorption in a single block is slight. The reflection coefficient of a mosaic crystal can be derived by analogy with Refs. 15 and 16 and in the Laue case it is described by

$$R_m^{s's} = \mu_d^{s's} \frac{\exp(D_1^{s's} t) - \exp(D_2^{s's} t)}{\gamma_1(D_1^{s's} - D_2^{s's})}, \quad (3)$$

where

$$D_{1,2}^{s's} = -\frac{1}{2} \left( \frac{\mu_2^{s's} + \mu_d^{s's}}{\gamma_2} + \frac{\mu_1^{s's} + \mu_d^{s's}}{\gamma_1} \right) \pm \left[ \frac{1}{4} \left( \frac{\mu_2^{s's} + \mu_d^{s's}}{\gamma_2} - \frac{\mu_1^{s's} + \mu_d^{s's}}{\gamma_1} \right)^2 + \frac{(\mu_d^{s's})^2}{\gamma_1 \gamma_2} \right]^{1/2};$$

$\mu_j^s = \kappa \text{Im}(F_{jj}^{ss})$  is the linear absorption coefficient of  $\gamma$  radiation with the  $s$  polarization in the course of propagation along a direction  $\mathbf{k}_j$ ;  $\mu_d^{s's} = \kappa \overline{|f_1|^2} F_{12}^{s's} F_{21}^{s's}$  is the coefficient representing the attenuation of the beam because of diffrac-

tion scattering; the factor  $\overline{|f_1|^2}$  depends on the size of the crystallites, their shape, and orientation. The bar denotes averaging of  $\overline{|f_1|^2}$  over the ensemble of the crystallites; for specific models we can calculate  $\overline{|f_1|^2}$  explicitly.

We shall consider the case of weak secondary extinction when the attenuation of a beam due to absorption in a crystal considerably exceeds the attenuation caused by diffraction scattering, i.e.,  $\mu_d^{s's} \ll \mu_1^s, \mu_2^s$  and we shall also assume that the inequality  $\mu_d^{s's} t / \gamma_{1,2} \ll 1$  is obeyed. In this case the reflection coefficient of Eq. (3) for the symmetric diffraction geometry ( $\gamma_1 = \gamma_2 = \gamma$ ) reduces to

$$R_m^{s's} = \frac{\mu_d^{s's}}{\mu_2^{s's} - \mu_1^{s's}} \left[ \exp\left(-\frac{\mu_1^{s's} + \mu_2^{s's}}{2\gamma} t\right) \right] \text{sh}\left(\frac{\mu_2^{s's} - \mu_1^{s's}}{2\gamma} t\right). \quad (4)$$

We shall point out that in Eq. (4) the reflection coefficient  $R_m^{s's}$  is proportional to  $\mu_d^{s's}$  and, consequently, to  $\overline{|f_1|^2}$ . This means that the dependence of  $R_m^{s's}$  on details of the mosaic can be ignored in comparing the theoretical and experimental spectra.

We investigated the influence of the interference between the  $c$  and  $d$  lines on the Laue diffraction spectra by numerical calculation of the spectra of Mössbauer  $\gamma$  radiation reflection by a system of (001) planes in a  $\text{Fe}_3\text{BO}_6$  crystal using the models of perfect and mosaic crystals. The results of the calculations carried out using Eqs. (1) and (4), averaged over the profile of the line of the source of  $\gamma$  rays, over the parameter  $\alpha$ , and over the polarization of  $\gamma$  rays are plotted in Fig. 3. The spectra in this figure have a number of properties in common and these reflect the characteristic features of the diffraction of  $\gamma$  rays in crystals in

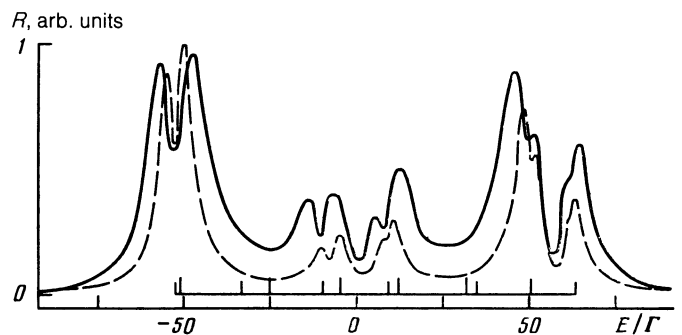


FIG. 3. Spectra of the (001) Laue reflection of Mössbauer  $\gamma$  radiation by  $\text{Fe}_3\text{BO}_6$  calculated for the models of perfect (continuous curve) and mosaic (dashed curve) crystals.

which the Mössbauer nuclei are at inequivalent positions, but the nature of the spectra is quite different for perfect and mosaic crystals.

The resonance peaks in the spectra in Fig. 3 are broadened and split, which is a consequence of the constructive interference of the  $c$  and  $d$  lines and of the resonance absorption of  $\gamma$  photons in a crystal. Moreover, in the case of a perfect crystal the broadening of the peaks and the presence of dips in the resonances can also be due to a suppression effect,<sup>6,7</sup> because  $F_{\text{str}}^c$  and  $F_{\text{str}}^d$  for the same nucleus are close to unity for the (001) reflection (Table I). Splitting of the resonance peaks appears most clearly for the sixth line in the spectrum when  $\Delta_i = |E_i^c - E_i^d|$  amounts to  $12\Gamma$ . The resonance peak for the sixth line is in the form of three well-resolved dips, two of which coincide in position with the resonant values of  $E_6^c$  and  $E_6^d$ , with the third located between the other two. The dip between the resonances is due to constructive interference between the  $c$  and  $d$  lines and is deepest for a given crystal thickness. In the case of the first, third, and fourth lines in the spectra of Fig. 3 the interference dips and the dips of the resonances cannot be resolved because  $\Delta_i$  is small ( $\leq 6\Gamma$ ).

The width of the resonance peaks in the (001) reflection spectrum and the magnitude of the splitting of these peaks in the case of a perfect crystal are significantly greater than for a mosaic crystal. The ratio of the intensities of the outer and inner lines in the spectrum is quite different for different models of a crystal: for a perfect crystal it is approximately twice as large. Moreover, the scattering intensity in the range of energies between the outer and inner resonance peaks of a perfect crystal is fairly high, whereas for a mosaic crystal it is close to zero. These differences between the spectra are due to the collective nature of the interaction of Mössbauer  $\gamma$  rays with a regular system of resonating nuclei<sup>1,6</sup> and can be used to obtain information on the degree of perfection of a given crystal when the theoretical and experimental spectra are compared.

### 3. EXPERIMENTAL METHOD

Interference effects in Laue diffraction were observed and the influence of a spin reorientation phase transition on the nature of the spectrum of reflected  $\gamma$  radiation was investigated using the apparatus shown schematically in Fig. 4. A beam of  $\gamma$  rays of  $0.5^\circ$  divergence emerging from a  $^{57}\text{Co}(\text{Cr})$  Mössbauer source 1, attached to a rod of an electrodynamic vibrator 2, reached a  $^{57}\text{Fe}_3\text{BO}_6$  single crystal 3 placed in a reflecting position. The activity of the source was  $\approx 10^{10}$  Bq and the energy width of the line was  $\Gamma_S = 2\Gamma$ . The crystal

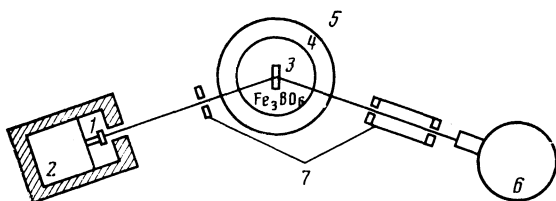


FIG. 4. Schematic diagram of the apparatus (explanations in text).

was in a thermal chamber 4 attached to a goniometer 5 and the scattered radiation was recorded using an Si:Li semiconductor detection unit 6. The background was minimized by a system of collimation slits 7.

The temperature in the chamber was maintained constant to within 0.01 K and the temperature drop across a sample was less than 0.1 K. These parameters were achieved as follows. The  $\text{Fe}_3\text{BO}_6$  crystal was placed in a beryllium capsule and attached at just one point to the capsule (in order to reduce deformation during heating) by a viscous contact paste (consisting of zinc oxide and silicone oil). This attachment method ensured reliable maintenance of the reflecting position of the crystal when the temperature in the chamber was increased from 293 to 520 K and, moreover, allowed us to minimize elastic stresses in the sample. The beryllium capsule with the crystal was attached to the wall of the chamber and was placed inside a heating element surrounded by thermal screening screens made of aluminum foil. The temperature in the chamber was maintained by a VRT-2 controller and two KhK<sub>68</sub> thermocouples. One thermocouple was placed alongside the heating element and it was included in the feedback loop of the VRT-2 controller, whereas the second thermocouple performed the monitoring function and was inside the capsule with the crystal. The second thermocouple was connected to a digital voltmeter with a printer output.

Measurements were made at two temperatures near the spin reorientation phase transition:  $T_1 = 410$  K and  $T_2 = 420$  K; a  $^{57}\text{Fe}_3\text{BO}_6$  single crystal of thickness  $15 \mu\text{m}$  was used. Heating of this crystal from  $T_1$  to  $T_2$  resulted in the rotation by  $90^\circ$  of the antiferromagnetic axis in the crystal, as described before, and it also altered the positions of the  $c$  and  $d$  resonance lines.<sup>17</sup> As shown later, these factors had a strong influence on the nature of the spectra of the diffracted  $\gamma$  radiation.

The nature of the spectrum of the Laue-diffracted radiation depended also on the value of the product  $\mu_N t$  for a crystal, where  $\mu_N$  is a resonance absorption coefficient of  $\gamma$  radiation by the nuclei. The values of  $\mu_N t$  for the sample used in our experiments were calculated for the  $\pi$  and  $\sigma$  polarizations of  $\gamma$  photons and are given in Table II for the  $(-3/2)-(-1/2)$  and  $(-1/2)-(-1/2)$  transitions representing the first and second resonance lines in the spectrum when the antiferromagnetic axis had the orientations corresponding to the temperatures  $T_1$  and  $T_2$ . The maximum values of  $\mu_N t$  given in Table II were of the order of 10, indicating that the investigated crystal was intermediate between "thin" ( $\mu_N t \leq 1$ ) and "thick" ( $\mu_N t \gg 10$ ) samples. In the case of such a crystal the suppression effect was less

TABLE II. Values of  $\mu_N t$  for the investigated crystal in the case of scattering involving  $(-3/2)-(-1/2)$  and  $(-1/2)-(-1/2)$  transitions by the  $^{57}\text{Fe}$  nuclei at the  $8d$  position.

Transition	$T < T_{SR}$		$T > T_{SR}$	
	$\pi$	$\sigma$	$\pi$	$\sigma$
$-3/2 - -1/2$	11.7	0	11.7	11.7
$-1/2 - -1/2$	0	15.4	0	0

strong than it would have been in the case of a thick crystal and, moreover, the diffracted radiation passed through the crystal even in the absence of the suppression effect.

#### 4. RESULTS OF EXPERIMENTAL INVESTIGATIONS: DISCUSSION

##### a) Spectra of purely nuclear reflections. Constructive interference

In an experimental study of the influence of the interference between the  $c$  and  $d$  lines on the nature of the Laue-diffraction energy spectra of the  $\text{Fe}_3\text{BO}_6$  crystal we selected the purely nuclear reflections (001) and (003). These reflections corresponded to the symmetric geometry of the diffraction experiment and the absence of the contribution of the Rayleigh scattering made it possible to investigate the interference between the  $c$  and  $d$  lines in its clearest form.

The selected reflections corresponded to the constructive interference between the  $c$  and  $d$  lines; the influence of this interference on the nature of the spectrum was discussed in detail above. Let us consider the nature of the spectra determined at the temperature  $T_2$  (Fig. 5). The resonance lines in the experimental spectra are broadened and split, which is manifested particularly strongly in the case of the first and sixth lines and, as pointed out, it may be a consequence of several factors: the interference between the  $c$  and  $d$  lines, the suppression of the inelastic channels, and the resonance absorption of  $\gamma$  radiation. In the case of the sixth line in both spectra (representing the  $3/2-1/2$ ) transition the split peak has three separate dips the deepest of which is the central one due to the interference attenuation of the beam intensity.

When we go over from the (001) to the (003) reflection, we find that the ratio of the intensities at the peak and in the dip of the split lines in the spectrum decreases, which is manifested most clearly in the case of the outer lines. This result is not evident *a priori* because an increase in the effective thickness of the crystal for higher reflection orders would seem to deepen the dips representing the absorption of  $\gamma$  rays. However, a reduction in the structure factors for the (003) reflection compared with the (001) case and the asso-

ciated attenuation of the scattering and interference between the  $c$  and  $d$  lines has a stronger influence on the profile of the resonance line and reduces the relative depth of the dip.

It should be pointed out that the (001) reflection spectrum does not have resonance dips for the transitions  $\Delta m = 0$  typical of the nuclear magnetic maxima (second and fifth lines in the spectrum); here,  $\Delta m$  is the difference between the magnetic quantum numbers for the ground and excited states of a nucleus.<sup>11</sup> The absence of these dips is due to the fact that the absorption coefficient  $\mu_N$  for the transition with  $\Delta m = 0$  is proportional to  $\sin^2\theta_B$  in the selected geometry and it is small. The resonance dips for these transitions are clearly visible in the (003) reflection spectrum because in this case the value of  $\mu_N$  for the transitions with  $\Delta m = 0$  is almost an order of magnitude greater than for the (001) reflection.

The experimental spectra of the (001) and (003) reflections measured at the temperature  $T_2$  are in good agreement with the theoretical spectra calculated for a perfect crystal. The slight difference between the theory and experiment (the dips are deeper at the resonances for the first and sixth lines in the experimental spectra compared with the corresponding dips in the theoretical spectra) is clearly due to the residual absorption of  $\gamma$  rays by the nuclei associated with imperfections of the investigated sample.

We shall now analyze the spectra measured at the temperature  $T_1$  (Fig. 6). In this case the positions of the resonance lines for the iron nuclei at the  $4c$  and  $8d$  positions is such that  $\Delta_i \lesssim 6\Gamma$ , so that in the case of the split outer lines in the spectrum there is only one dip and the inner lines are not split. The spectra of the (001) and (003) reflections near the resonance transitions characterized by  $\Delta m = \pm 1$  are in good agreement with the numerical calculations carried out for a perfect crystal. However, near the  $\Delta m = 0$  transitions there is a qualitative difference between the theory and experiment. The theoretical spectra calculated allowing only for the magnetic structure have dips near these transitions, due to the absorption of  $\gamma$  rays, whereas the experimental spectra have clear peaks which, as shown in Ref. 11, are due to the combined hyperfine interaction in the  $\text{Fe}_3\text{BO}_6$  crystal

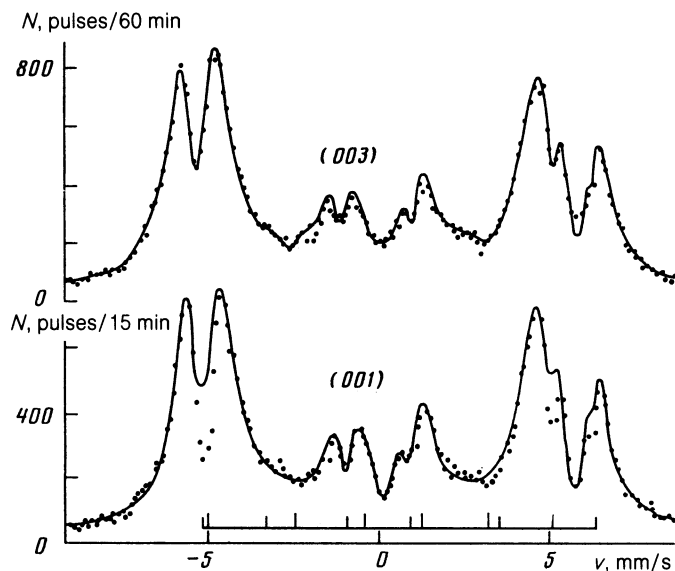


FIG. 5. Spectra of the (001) and (003) reflections of Mössbauer  $\gamma$  radiation by a  $\text{Fe}_3\text{BO}_6$  crystal determined at  $T_2 = 420$  K. The continuous curves are the theoretical spectra calculated for the model of a perfect crystal; the Bragg angle  $\theta_B$  was  $5.54^\circ$  for the (001) reflection and  $16.8^\circ$  for the (003) reflection.

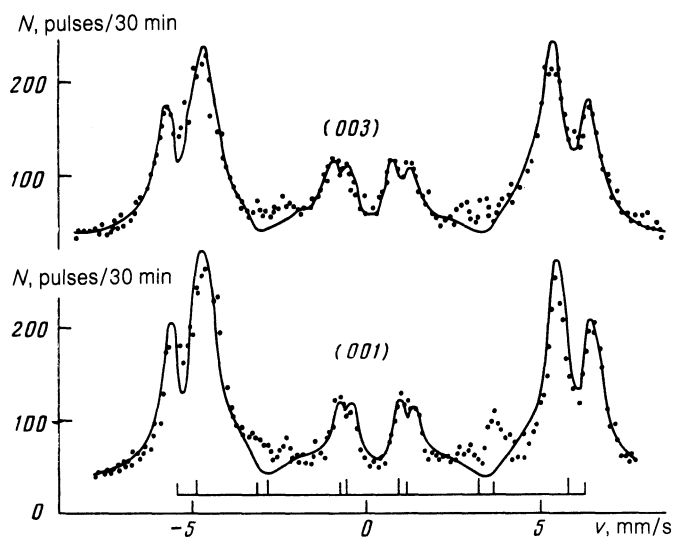


FIG. 6. Spectra of the (001) and (003) reflections measured at  $T_1 = 410$  K.

(combined peaks). In general, the combined structure of the hyperfine fields influences all the transitions between the Zeeman sublevels of the ground and excited states of a nucleus and in this sense all the resonance peaks in the spectra of Figs. 5 and 6 are combined, but we shall restrict the term "combined" only to the peaks corresponding to the second and fifth resonance lines, because in their case the combined nature of the hyperfine interactions is manifested most clearly.

Such peaks can occur as a result of the scattering of Mössbauer radiation in crystals in which the structures due to the magnetic and electric fields are of different symmetry, as predicted in Ref. 9. The physical reason for the appearance of these peaks in the case of purely nuclear reflection of Mössbauer radiation is as follows: when the Mössbauer nuclei are subject to a magnetic field  $\mathbf{H}$  and to a nonaxisymmetric EFG tensor, the principal axes of which do not coincide with  $\mathbf{H}$ , the eigenvectors of the hyperfine interaction Hamiltonian are not pure states with a specific value of  $m$  but are superpositions of these states. Moreover, the appearance of combined peaks may result from the difference between the orientations of the EFG axes at nuclei with the antiparallel orientation of  $\mathbf{H}$  at each of the inequivalent positions. For these reasons the amplitudes of the scattering by the Mössbauer nuclei with the antiparallel orientations of  $\mathbf{H}$  are not equal, which is the reason for the appearance of the peaks in the case of the second and fifth lines in the spectra of purely nuclear magnetic reflections.

The intensity of the combined peaks depends on the magnetic and quadrupole interactions, and also on the mutual orientation of the magnetic fields, the principal axes of the EFG tensor, and the vectors  $\mathbf{k}_1$  and  $\mathbf{k}_2$ . In the case when the structure of hyperfine fields in a crystal is not known, the energy spectra of purely nuclear reflections containing resonance peaks due to transitions characterized by  $\Delta m = 0$  can be calculated numerically as was done, for example, in the case of an yttrium iron garnet crystal in Ref. 18.

An analysis of the spectra shown in Fig. 6 demonstrates that the intensities of the peaks due to the transitions with  $\Delta m = 0$  are less for the (003) reflection than for the (001) case, and in both spectra the peak for the fifth line is clearer than for the second, which is obviously due to the character-

istic features of the interference between the  $c$  and  $d$  lines.

The presence of combined resonance peaks in the spectra determined at  $T < T_{SR}$  and their absence (within the limits of the experimental error) at  $T > T_{SR}$  may be due to the orientational dependence of the intensities of the combined peaks discussed above. The reason for the reduction in the intensity of these peaks in the (003) reflection spectrum, compared with the (001) spectrum, may be due to a difference between the angles separating the axes of the hyperfine interactions in the investigated crystals from the vectors  $\mathbf{k}_1$  and  $\mathbf{k}_2$  for these two reflections, and it may also be due to changes in the corresponding structure factors.

#### b) Interference between nuclear and Rayleigh scattering

We considered earlier the interference between the  $c$  and  $d$  lines in the scattering of Mössbauer  $\gamma$  radiation by a  $\text{Fe}_3\text{BO}_6$  crystal into purely nuclear diffraction maxima for which the electron component of the scattering amplitude  $F_{(r)ij}^{s_s}$  ( $i \neq j$ ) of Eq. (2) vanishes. However, in the case of an arbitrary  $(hkl)$  direction the amplitude of the scattering by electrons does not vanish so that in discussing resonant scattering of  $\gamma$  radiation in this crystal we must consider not only the interference between the  $c$  and  $d$  lines, but also the interference between the radiation scattered by the nuclei and by the electrons, which can alter significantly the spectra of the diffracted  $\gamma$  radiation compared with the case of pure nuclear scattering. In this section we shall consider the influence of the interference between nuclear and Rayleigh (electron) scattering processes on the Laue diffraction spectra in the case of the (002) reflection. The results of the measurements are presented in Fig. 7.

The (002) reflection is characterized by the constructive interference between the  $c$  and  $d$  lines, which broadens the resonance line in the spectrum. The Rayleigh scattering by electrons of amplitude which is not small compared with the nuclear process has the effect that the interference between the  $c$  and  $d$  lines is weaker than in the pure nuclear scattering case, in particular, it may result in the absence of interference attenuation of the intensity of the diffracted beam. The intensity of the reflected radiation considered as a function of the  $\gamma$ -photon energy is of dispersive form, typical of interference between the nuclear and Rayleigh scattering

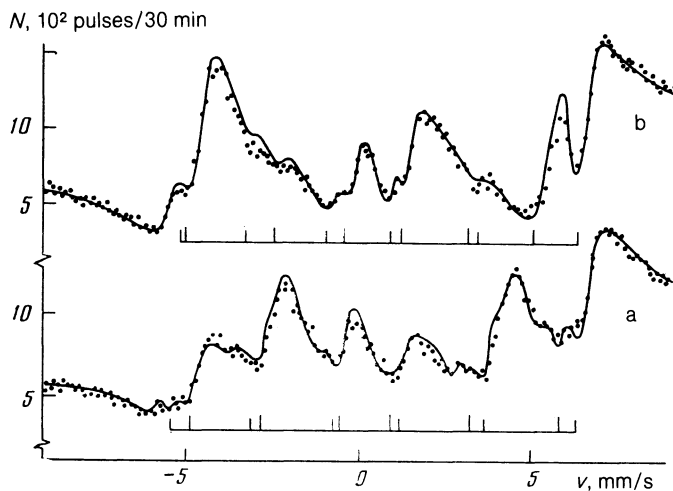


FIG. 7. Spectra of the (002) reflection of Mössbauer  $\gamma$  radiation by a  $\text{Fe}_3\text{BO}_6$  crystal determined at the following temperatures: a)  $T = T_1$ ; b)  $T = T_2$ ;  $\theta_B = 11.1^\circ$ . The continuous curves are the theoretical spectra calculated in the model of a perfect crystal.

processes, reaching a minimum at the resonances (or to the left of them) and a maximum to the right of the resonances.

When the orientation of the antiferromagnetic axis corresponds to the temperature  $T_1$  (Fig. 7a), the spectrum includes all the resonance lines and the strongest scattering occurs for the  $\Delta m = 0$  transitions. Above the phase transition point  $T_{SR}$  the orientation of the antiferromagnetic axis is such (Fig. 2a) that the strongest scattering is that due to the  $\Delta m = \pm 1$  transitions and the scattering due to the  $\Delta m = 0$  transitions is practically absent (Fig. 7b).

### c) Destructive interference of the $c$ and $d$ lines

The experimental spectra discussed above correspond to constructive interference between the  $c$  and  $d$  lines. Figure 8 shows the (080) reflection spectra corresponding to destructive interference, determined at temperatures  $T_1$  and  $T_2$ .

We shall first consider the (080) reflection spectrum determined at  $T_2$  (Fig. 8b). The orientation of the antiferromagnetic axis in this case is such that the amplitude of the nuclear resonance scattering  $F_{(N)}$  for the  $\Delta m = \pm 1$  transitions is high and it exceeds considerably the amplitude of the scattering by electrons  $F_{(R)}$ , so that interference between the nuclear and Rayleigh processes of the scattering of  $\gamma$  radiation has little influence on the nature of the spectrum and

the interference between the  $c$  and  $d$  resonance lines plays the major role. The strongest peak in this spectrum is the resonance corresponding to the sixth line and the intensities of the other peaks are considerably less. Such a difference between the peak intensities is due to the fact that the sixth line corresponds to a larger width  $\Delta_i$  manifesting a strong interference enhancement of the diffracted beam. In the case of the remaining  $\Delta m = \pm 1$  transitions the separation between the  $c$  and  $d$  lines is small, so that in their case the destructive interference effects result mainly in the weakening of the resonance peak intensities. The amplitude of the resonant nuclear scattering via the  $\Delta m = 0$  transitions is proportional to the factor  $\sin^2\theta_B$  the value of which is 0.16 for the (080) reflection, so that the intensities of the peaks are lowest for the second and fifth lines in the spectrum.

It should be pointed out that in the case of the (080) reflection when the orientation of the antiferromagnetic axis corresponds to the temperature  $T_2$ , we can expect almost complete suppression if we ignore the Rayleigh scattering in a crystal. In the case of the scattering as a result of the  $\Delta m = \pm 1$  transitions the suppression affects the  $\pi$ - and  $\sigma$ -polarized  $\gamma$  rays, whereas in the case of the  $\Delta m = 0$  transitions this is only true of the  $\sigma$ -polarized rays (because the  $\pi$ -polarized  $\gamma$  photons do not interact with nuclei in this transitions), which again weakens the resonance peaks corresponding to the second and fifth lines.

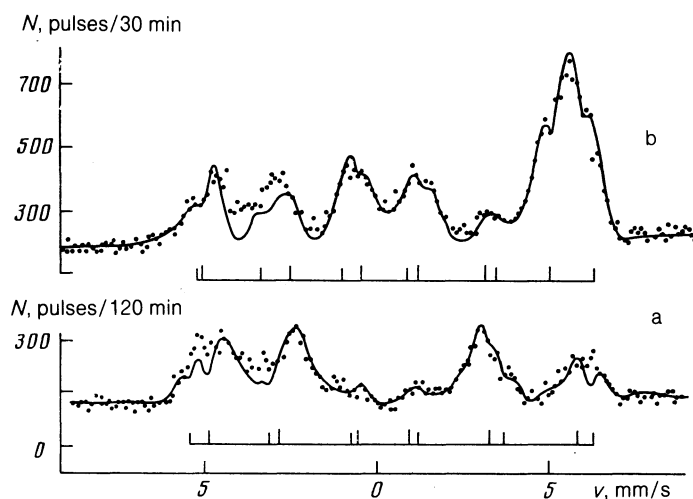


FIG. 8. Spectra of the (080) reflection determined at: a)  $T = T_1$ ; b)  $T = T_2$ ;  $\theta_B = 23.8^\circ$ .

The resonance peak for the sixth line is of "three-hump" nature with the strongest central maximum, and the dips between the humps correspond to the resonance energies  $E_6^c$  and  $E_6^d$  and are due to, as in the case of purely nuclear scattering discussed earlier, the influence of a residual absorption in a crystal and of the suppression effect. The experimental spectrum shown in Fig. 8b is in good agreement with theoretical calculations for a perfect crystal.

It follows from the results obtained that in the case of diffraction of Mössbauer  $\gamma$  radiation in a  $\text{Fe}_3\text{BO}_6$  crystal we can expect the destructive interference between the  $c$  and  $d$  lines to enhance the intensity of the diffracted  $\gamma$ -photon beam and, consequently, to produce interference bleaching of a crystal for the resonant  $\gamma$  radiation. It follows from numerical calculations that this result is not affected qualitatively by an increase in the crystal thickness. The physical reason for the enhancement of the intensity of the diffracted beam is that, because of the interference between the  $c$  and  $d$  lines, the reflection and absorption maxima of resonance  $\gamma$  photons occur at different values of the  $\gamma$ -photon energy. It should be stressed that the interference enhancement of the intensity of a  $\gamma$ -ray beam transmitted by a crystal under Laue diffraction conditions occurs not only in the case of a perfect crystal, but also in the case of a mosaic crystal.

The (080) reflection spectrum determined at the temperature  $T_1$  is shown in Fig. 8a. The orientation of the antiferromagnetic axis corresponding to this case is shown in Fig. 2b. The spectrum differs considerably from that determined at the temperature  $T_2$  and shown in Fig. 8b, and the difference is due to several factors. One of them is the change in the separation between the  $c$  and  $d$  lines as a result of the transition across the temperature  $T_{\text{SR}}$ . Since at  $T_1$  this separation is less than  $6\Gamma$ , the interference enhancement of the intensity of the diffracted beam is manifested less strongly. The other factor is that in the selected geometry the suppression effect applies only to the  $\Delta m = 0$  transitions (in the case of  $\pi$ -polarized  $\gamma$  rays). These factors have the effect that the intensity of the resonance peaks in the spectrum is considerably less than in the spectrum of Fig. 8b. The (080) reflection spectrum determined at the temperature  $T_1$  is in agreement with the results of numerical calculations carried out using a model of a perfect crystal. By analogy with the (001) and (003) reflection spectra at temperatures  $T < T_{\text{SR}}$  (Fig. 5), the difference between the theoretical and experimental results may be due to the dependence of the amplitude of Eq. (2) on the EFG, which is ignored in the calculations.

## 5. CONCLUSIONS

The results obtained in the present study reveal a number of interesting and important properties of diffraction scattering of Mössbauer  $\gamma$  radiation in a  $\text{Fe}_3\text{BO}_6$  crystal and, in a more general sense, in crystals in which the resonant nuclei occupy crystallographically inequivalent positions. It is shown that the interference between the  $c$  and  $d$  resonance lines alters greatly the energy spectrum of the Laue-diffracted radiation compared with the case when the Mössbauer nuclei occupy equivalent positions in a crystal and, depending on the nature of the interference process, we can expect interference attenuation or enhancement of the intensity of the diffracted beam. Our study of the influence of the Rayleigh scattering of  $\gamma$  photons on the interference between the  $c$  and  $d$  lines demonstrated in particular that the Rayleigh

scattering may result in "smearing" of the interference pattern of the spectrum due to the scattering by nuclei.

Experimental investigations were made of combined peaks in the diffracted radiation spectrum due to the existence of a combined hyperfine interaction in a  $\text{Fe}_3\text{BO}_6$  crystal and an analysis was carried out of the possible reasons for changes in the intensity of these peaks as a result of changes in the orientation of the antiferromagnetic axis in a crystal, and also due to a change from one reflection to another. It should be pointed out that the presence of combined peaks in the diffraction spectrum is a specific feature of the scattering of Mössbauer  $\gamma$  radiation and has no analogs in the scattering of other radiations. Moreover, the interference enhancement of the intensity of the diffracted beam as a result of the destructive interference of the  $c$  and  $d$  lines (interference bleaching of a crystal), discovered for the first time in the present study, is also important. It should be pointed out that this effect increases the transparency of crystals and it is particularly interesting in the case of mosaic samples which do not exhibit the suppression effect.

The results of the present study can be used in investigations of the structure of crystals by Mössbauer diffraction, particularly in determination of the structure of the EFGs in a  $\text{Fe}_3\text{BO}_6$  crystal, and also in studies of spin-reorientation phase transitions, including the structure in the direct vicinity of  $T_{\text{SR}}$ . The differences between the interference patterns of perfect and mosaic crystals can, in principle, be used to study the degree of perfection of crystals.

The authors are grateful to A. N. Artem'ev, V. E. Dmitrienko, and G. V. Smirnov for valuable discussions.

<sup>1</sup>We shall use here a classification of the transitions corresponding to the magnetic hyperfine interaction.

<sup>1</sup>Yu. Kagan and A. M. Afanas'ev, in: Mössbauer Spectroscopy and Its Applications (Proc. Panel Meeting, Vienna, 1971), International Atomic Energy Agency, Vienna (1972), p. 143.

<sup>2</sup>A. N. Artem'ev, I. P. Perstnev, V. V. Sklyarevskii, G. V. Smirnov, and E. P. Stepanov, Zh. Eksp. Teor. Fiz. **64**, 261 (1973) [Sov. Phys. JETP **37**, 136 (1973)].

<sup>3</sup>E. P. Stepanov, A. N. Artem'ev, I. P. Perstnev, V. V. Sklyarevskii, and G. V. Smirnov, Zh. Eksp. Teor. Fiz. **66**, 1150 (1974) [Sov. Phys. JETP **39**, 562 (1974)].

<sup>4</sup>P. P. Kovalenko, V. G. Labushkin, A. K. Ovsepyan, É. R. Sarkisov, and E. V. Smirnov, Pis'ma Zh. Eksp. Teor. Fiz. **39**, 471 (1984) [JETP Lett. **39**, 573 (1984)].

<sup>5</sup>P. P. Kovalenko, V. G. Labushkin, A. K. Ovsepyan, É. R. Sarkisov, E. V. Smirnov, and I. G. Tolpekin, Zh. Eksp. Teor. Fiz. **88**, 1336 (1985) [Sov. Phys. JETP **61**, 793 (1985)].

<sup>6</sup>A. M. Afanas'ev and Yu. Kagan, Zh. Eksp. Teor. Fiz. **64**, 1958 (1973) [Sov. Phys. JETP **37**, 987 (1973)].

<sup>7</sup>G. V. Smirnov, V. V. Mostovoi, Yu. V. Shvyd'ko, V. N. Seleznev, and V. V. Rudenko, Zh. Eksp. Teor. Fiz. **78**, 1196 (1980) [Sov. Phys. JETP **51**, 603 (1980)].

<sup>8</sup>U. van Bürck, G. V. Smirnov, H. J. Maurus, and R. L. Mössbauer, J. Phys. C **19**, 2557 (1986).

<sup>9</sup>A. V. Kolpakov, E. N. Ovchinnikova, and R. N. Kuz'min, Vestn. Mosk. Univ. Fiz. Astron. **33**, No. 2, 28 (1978).

<sup>10</sup>A. V. Kolpakov, E. N. Ovchinnikova, and R. N. Kuzmin, Phys. Status Solidi B **93**, 511 (1979).

<sup>11</sup>I. G. Tolpekin, P. P. Kovalenko, V. G. Labushkin, E. N. Ovchinnikova, É. R. Sarkisov, and E. V. Smirnov, Pis'ma Zh. Eksp. Teor. Fiz. **43**, 474 (1986) [JETP Lett. **43**, 610 (1986)].

<sup>12</sup>O. A. Bayukov, V. M. Buznik, V. P. Ikonnikov, and M. I. Petrov, Fiz. Tverd. Tela (Leningrad) **18**, 2319 (1976) [Sov. Phys. Solid State **18**, 1353 (1976)].

<sup>13</sup>E. V. Smirnov and V. A. Belyakov, Zh. Eksp. Teor. Fiz. **79**, 883 (1980) [Sov. Phys. JETP **52**, 448 (1980)].

<sup>14</sup>Z. G. Pinsker, *X-Ray Crystal Optics* [in Russian], Nauka, Moscow (1982).

<sup>15</sup>Yu. Kagan, A. M. Afanas'ev, and I. P. Perstnev, Zh. Eksp. Teor. Fiz. **54**, 1530 (1968) [Sov. Phys. JETP **27**, 819 (1968)].

<sup>16</sup>V. E. Dmitrienko and V. A. Belyakov, Acta Crystallogr. Sect. A **36**, 1044 (1980).

<sup>17</sup>O. A. Bayukov, V. P. Ikonnikov, M. I. Petrov, V. N. Seleznev, R. P. Smolin, and V. V. Uskov, Pis'ma Zh. Eksp. Teor. Fiz. **14**, 49 (1971)

[JETP Lett. **14**, 32 (1971)].

<sup>18</sup>H. Winkler, R. Eisberg, E. Alp, R. Ruffer, E. Gerdau, S. Lauer, A. X. Trautwein, M. Grodzicki, and E. Vera, Z. Phys. B **49**, 331 (1983).

Translated by A. Tybulewicz